Vol. 135: 107–119, 2019
https://doi.org/10.3354/dao03390

DISEASES OF AQUATIC ORGANISMS
Dis Aquat Org

Published online July 25

Investigating the natural resistance of blackfoot pāua *Haliotis iris* to abalone viral ganglioneuritis using whole transcriptome analysis

Matthew J. Neave, Serge Corbeil*, Kenneth A. McColl, Mark St. J. Crane

Australian Animal Health Laboratory, Private Bag 24, Geelong, VIC 3220, Australia

ABSTRACT: The natural resistance of New Zealand blackfoot pāua *Haliotis iris* to infection by haliotid herpesvirus-1 (HaHV-1) and to the disease abalone viral ganglioneuritis was investigated in experimentally challenged pāua using high throughput RNA-sequencing. HaHV-1-challenged pāua up-regulated broad classes of genes that contained chitin-binding peritrophin-A domains, which seem to play diverse roles in the pāua immune response. The pāua also up-regulated vascular adhesion protein-1 (VAP-1), an important adhesion molecule for lymphocytes, and chitotriosidase-1 (CHIT-1), an immunologically important gene in mammalian immune systems. Moreover, several blood coagulation pathways were dysregulated in the pāua, possibly indicating viral modulation. We also saw several indications that neurological tissues were specifically affected by HaHV-1, including the dysregulation of beta-1,4-N-acetylgalactosaminyltransferase (B4GALNT), GM2 ganglioside, neuroligin-4 and the Notch signalling pathway. This research may support the development of molecular therapeutics useful to control and/or manage viral outbreaks in abalone culture.

KEY WORDS: Pāua · Abalone · Haliotid herpesvirus · HaHV-1 · Transcriptome · Peritrophin-A · RNA-Seq

1. INTRODUCTION

Since the early 2000s, haliotid herpesvirus 1 (HaHV-1; formerly abalone herpesvirus, AbHV-1), the aetiological agent of the disease abalone viral ganglioneuritis (AVG), has caused significant financial losses to the wild fisheries and land-based aquaculture industry in Taiwan and Australia (Wang et al. 2004, Chang et al. 2005, Hooper et al. 2007). For more than a decade, studies have been conducted to characterize the virus at structural and molecular levels (Chang et al. 2005, Hooper et al. 2007, Tan et al. 2008, Savin et al. 2010, Cowley et al. 2012, Crane et al. 2013) as well as at the epidemiological (Corbeil et al. 2012a,b) and immunological levels (Dang et al. 2013). In addition, previous studies have shown that *Haliotis diversicolor* Reeve 1846 and *H. diversicolor supertexta* as well as *H. conicopora, H. rubra*, *H. laevigata* and the hybrid *H. rubra* × *H. laevigata* are all susceptible to infection by HaHV-1 and to the disease AVG (Wang et al. 2004, Chang et al. 2005, Corbeil et al. 2016, Bai et al. 2019). However, a recent study by Corbeil et al. (2017) has identified an abalone species (blackfoot pāua *H. iris,* hereafter pāua) from New Zealand that is both highly resistant to virus infection and to disease. Knowledge of mollusc immune responses to pathogen infections is still scarce; however, in the past 15 yr, studies investigating genomics, proteomics, cell signalling pathways, antimicrobial peptides, microRNAs and RNA interference in oysters, scallops, mussels and abalone have provided invaluable information on defence mechanisms of these invertebrate species (Canesi et al. 2003, Fleury & Huvet 2012, Chen et al. 2013, 2014, 2015, Corporeau et al. 2014, Martín-Gómez et

*Corresponding author: s.corbeil@csiro.au

al. 2014, Normand et al. 2014, Green et al. 2015a,b, He et al. 2015, Rosani et al. 2015, Zhuang et al. 2015, Seo et al. 2016, Gerdol et al. 2018, Bai et al. 2018). The mechanisms of resistance of pāua to AVG are not yet known. In this study, we used a next-generation sequencing approach to unveil some of the mysteries associated with this phenomenon.

2. MATERIALS AND METHODS

2.1. Experimental animals

Pāua *Haliotis iris* (50 mm in length) were imported from Moana New Zealand Blue abalone Ltd (Northland, New Zealand). As positive controls to validate the infectivity process, healthy susceptible blacklip *H. rubra* × greenlip *H. laevigata* abalone hybrids (50 mm in length) were obtained from the abalone farm Craig Mostyn Group Jade Tiger Abalone Pty Ltd (Indented Head, Victoria, Australia) where there has been no history of AVG. For all experiments, single abalone were placed in individual 2 l aquaria each containing 1 l of aerated, filtered natural seawater (salinity 35‰) maintained at 16 ± 1°C. Air-conditioning was used to maintain a constant room temperature. During each experiment, abalone were fed artificial pellets (Halo, Skretting), and each aquarium underwent a 100% water change every 2 d.

2.2. Production of HaHV-1 infectious water

We followed the experimental procedure described by Corbeil et al. (2017). In brief, infectious water for immersion challenges was produced by intramuscularly injecting 30 naïve hybrid abalone with 100 µl of HaHV-1 stock solution. Injected abalone were held in tanks containing 20 l aerated sea water (changed daily). On Day 4 post injection, water was harvested to provide the immersion challenge dose (1:2 dilution).

2.3. Immersion challenge and tissue harvesting

Challenges were performed in 2 l tanks for 20 h by exposing 9 pāua individually to 1 l of HaHV-1 infectious water. Negative control groups (8 pāua and 8 hybrid abalone) were exposed to seawater. After 24 h, the infectious water was replaced with 2 l of fresh seawater. At 24 and 96 h post challenge, replicate pāua were sampled. The gills and surrounding tissues (osphradium, nephridium, mantle and associated haemocytes) were removed, stored in RNA*later*® solution for 24 h and then frozen at −20°C until processing (library and sequencing) (2× 24 h controls, 2× 96 h controls, 2× 24 h challenged and 3× 96 h challenged; see Fig. 2). Thus, 9 pāua in total were used for RNA-sequencing (RNA-Seq). Nerve tissues and associate musculature were harvested and directly frozen at −20°C until processing for viral quantitation. Because the gills are a natural route of infection for pathogens, it is likely that variation in gene expression would be detected in these tissues.

2.4. Viral load quantitation

Viral load (expressed as viral gene copy numbers per mg of abalone tissue), from pooled tissues (nerves with some associated muscle) of challenged pāua and pooled tissues of hybrid abalone from time point 96 h was determined using qPCR and a standard curve, as described previously (Corbeil et al. 2010), but using the primers and probe ORF-66 described by OIE (2017). Briefly, the ORF-66 plasmid containing the virus target gene was serially diluted in water and run in parallel to extracted tissue DNA samples. A linear correlation was obtained between template copy number and the cycle threshold value from over 4 $\log_{10}$ dilutions.

2.5. RNA extraction and sequencing

Total RNA was extracted from tissues using the RNeasy Kit (Qiagen) following the manufacturer's instructions. Quantitation of RNA samples was performed on the 2100 Bioanalyser using RNA Nano Chips (Agilent Technologies). RNA-Seq was conducted on 9 pāua samples: 2× 24 h controls, 2× 96 h controls, 2× 24 h HaHV-1 challenged and 3× 96 h HaHV-1-challenged. The RNA samples were sent to the Australian Genome Research Facility (Melbourne), where messenger RNA (mRNA) was enriched in each sample using polyA+ selection, which was then sequenced using one 125-bp paired-end HiSeq lane (Illumina). Raw RNA-Seq reads have been deposited in the NCBI Sequence Read Archive under BioProject accession PRJNA445893.

2.6. Data analysis

Trimmomatic v.0.36 (Bolger et al. 2014) was used to remove Illumina adapters, trim sequences with qual-

ity less than 20 and remove reads less than 100 bp. Ribosomal RNA (rRNA) that survived the polyA+ enrichment process was then removed *in silico* by mapping the cleaned reads to a database containing all *Haliotis* rRNA in the NCBI non-redundant (nr) database (Benson et al. 2013) (accessed 06.04.2019) using Bowtie v.2.2.9 (Langmead & Salzberg 2012) and SAMtools v.1.3.1 (Li et al. 2009). The high-quality mRNA reads from each sample were then combined, and a pāua reference transcriptome was assembled using Trinity v.2.3.2 (Haas et al. 2013) with a minimum k-mer coverage of 2 and digital normalization enabled. The assembly quality and gene expression distribution were assessed using scripts available in the Trinity installation. For annotation of the reference transcriptome, we used the Trinotate pipeline v.3.0.2 (Grabherr et al. 2011), which included BLASTP and BLASTX searches (Altschul et al. 1990) against the UniProt database (The UniProt Consortium 2017), and HMMER searches (Johnson et al. 2010) against the Pfam protein family database (Punta et al. 2012). Both databases were accessed on 06.04.2019. In addition, BLASTP (Altschul et al. 1990) was used to compare the predicted proteins to the NCBI nr database (Benson et al. 2013) accessed on 06.04.2019.

To estimate expression abundance, the reads from individual pāua samples were aligned to the reference transcriptome using 'align_and_estimate_abundance.pl' within Trinity v.2.3.2 (Haas et al. 2013), using RSEM v.1.2.31 (Li & Dewey 2011) for abundance estimation and Bowtie v.2.2.9 (Langmead & Salzberg 2012) for alignment. The counts were then tested for differential gene expression between HaHV-1-challenged pāua and the controls using 'run_DE_analysis.pl' with edgeR (Robinson et al. 2010) and a false discovery rate corrected p-value of 0.01, and tests for gene ontology enrichment enabled (Haas et al. 2013). The figures for transcriptome quality and differential expression analysis were produced using ggplot v.2.2.1 (Wickham 2016).

2.7. Clustering predicted proteins

To determine genetic similarities between pāua and other *Haliotis* species, we clustered the predicted pāua proteins with predicted proteins from *H. discus hannai* (Nam et al. 2017) and *H. laevigata* (N. Botwright unpubl. data).

Low-quality predicted proteins (shorter than 10 amino acids or with more than 20% stop codons) were removed from the analysis. The remaining proteins were compared to each other using orthoMCL v.2.0.9 (Li et al. 2003) to determine homologous genes between the species. A Venn diagram depicting common and unique genes was constructed using orthomclToVenn v.1.0 (Bayer 2017) and Matplotlib v2.0.2 (Hunter 2007).

2.8. Phylogenetic analysis of chitin-binding peritrophin-A domains

Chitin-binding peritrophin-A domains were frequently detected in the differentially expressed genes, and for this reason, they were analysed further. A custom Python v.3.5.2 script was used to extract these domains from the transcripts if they had an expression of 1 count per million in at least 2 replicates. In addition, the chitin-binding peritrophin-A domains were required to have the following structure: $CX_{17-20}CX_5CX_{7-22}CX_{12}CX_{6-16}C$, where C indicates conserved cysteine residues, X indicates any amino acid, and the subscript values indicate the number of spacing residues (Tetreau et al. 2015). Domains meeting these requirements were then aligned using MUSCLE v.3.8.31 (Edgar 2004) with the default settings. A phylogenetic tree was created from the alignment using RAxML (Stamatakis 2014) with 1000 bootstrap replicates and the 'PROTGAMMAWAG' model, and exported to GGTREE v.1.8.2 (Yu et al. 2017) for annotation with expression values.

3. RESULTS

3.1. Viral challenge

Quantitative PCR performed on gill and surrounding tissues (e.g. osphradium, nephridium, mantle, haemocytes) as well as nerve and associated abalone tissues from HaHV-1-challenged pāua and hybrid abalone indicated that the pāua had no viral DNA. On the other hand, the susceptible positive control hybrid abalone had a titre of 375 viral gene copies mg^{-1} of tissue (96 h post challenge), confirming that the viral challenge was successful.

3.2. Pāua transcriptome assembly and annotation

More than 35 million raw RNA-Seq reads were generated for each pāua sample (Table 1). Following stringent quality trimming and ribosomal RNA removal, approximately 70% of the reads remained for most samples (Table 1). However, the reads for 2 of

Table 1. Experimental design and RNA-Seq read quality, including the number of samples, treatment type, number of raw RNA-Seq reads obtained, number of RNA-Seq reads remaining after trimming and number of RNA-Seq reads remaining after removing ribosomal RNA. Numbers in brackets are the percentages of reads retained

Sample	Virus	Hours post infection	Number of raw reads	Number of quality trimmed reads	Number of reads after ribosomal RNA removal
C	HaHV-1	24	36 385 660	19 751 516 (54.3)	19 639 717 (99.4)
D	HaHV-1	24	50 929 696	35 612 010 (69.9)	31 415 239 (88.2)
E	HaHV-1	96	41 258 386	31 302 317 (75.9)	31 195 053 (99.7)
F	HaHV-1	96	42 282 446	29 881 346 (70.7)	28 945 019 (96.9)
H	HaHV-1	96	43 502 192	32 572 657 (74.9)	32 400 925 (99.5)
I	Control	24	37 497 364	15 399 332 (41.1)	15 131 920 (98.3)
J	Control	24	44 284 146	32 962 127 (74.4)	32 872 400 (99.7)
N	Control	96	47 363 128	33 878 349 (71.5)	32 726 069 (96.6)
O	Control	96	44 064 948	34 515 238 (78.3)	34 342 897 (99.5)

the samples (C and I in Table 1) were reduced to 54 and 41%, respectively, due to the formation of 'primer dimers' (Table 1). Nevertheless, at least 15 million high-quality reads were obtained for each of these samples, ensuring adequate transcriptome coverage (Table 1).

The high-quality reads from each pāua were combined and assembled into a pāua transcriptome containing 141 626 genes and 186 507 transcripts, although only 14 036 transcripts were responsible for 90% of all expression. The transcriptome assembly quality was assessed using the 'expression N50' (ExN50), which is a variation of the more common 'contig N50'. The ExN50 can be considered a more appropriate metric for transcriptome quality due to the large dynamic range of expression values and the generation of transcript isoforms (Haas et al. 2013; http://trinityrnaseq.github.io). For the pāua transcriptome, the ExN50 was 1492 bp and the peak approached an expression percentile of 100 (Fig. 1a), suggesting that deeper sequencing would not recover a significant number of new transcripts or provide a higher-quality assembly.

To determine the annotation sources for the pāua transcriptome, taxa with the best matching transcripts in the NCBI nr database were extracted and tallied (Fig. 1b). As expected, the majority of transcripts were annotated using taxa from the phylum Mollusca and the classes Gastropoda and Bivalvia (Fig. 1b), closely matching pāua taxonomy. At the family level, a number of annotations were acquired from Lottiidae (limpets), Ostreidae (oysters), Pectinidae (scallops) and Aplysiidae (sea hares) (Fig. 1b). The Haliotidae (which includes pāua) contributed approximately 8% of the annotations (Fig. 1b), probably reflecting the relatively limited number of pāua and abalone sequences in reference databases at the time annotation was performed.

The pāua transcriptome was also compared to other publicly available *Haliotis* transcriptomes, including those of *H. discus hannai* and *H. laevigata*. The transcriptomes from these species were clustered to reveal homologous transcripts between the species (Fig. 1c). All 3 species were predicted to share more than 26 000 transcript clusters, with several thousand transcripts also uniquely shared between any 2 of the species (Fig. 1c). In addition, from 15 810 (*H. discus hannai*) to 33 438 (*H. iris*) transcript clusters were unique to a particular species (Fig. 1c).

3.3. Pāua gene expression changes following HaHV-1 infection

Pāua challenged with HaHV-1 had distinct gene expression profiles compared to the control pāua, and the time post-exposure (24 vs. 96 h) also influenced the gene expression profiles (Fig. 2a,b). Although the replicates within each treatment grouped together, there was significant intra-treatment variability, particularly for the control time-points and HaHV-1-challenged pāua after 24 h (Fig. 2a,b). Nevertheless, we were able to use the specific differences between control and HaHV-1-challenged pāua to examine differentially expressed genes that may be a direct response to the viral infection (Fig. 2c).

At 24 h post-exposure, the pāua differentially expressed 375 genes (323 up-regulated and 52 down-regulated), and this increased to 887 genes (320 up-regulated and 567 down-regulated) after 96 h (Fig. 2c). The most differentially expressed genes 24 h post-exposure were frequently involved in chitin-binding, or contained chitin-binding peritrophin-A domains (pfam 01607), such as endochitinases, protein PIF and 2 protein obstructor-E genes

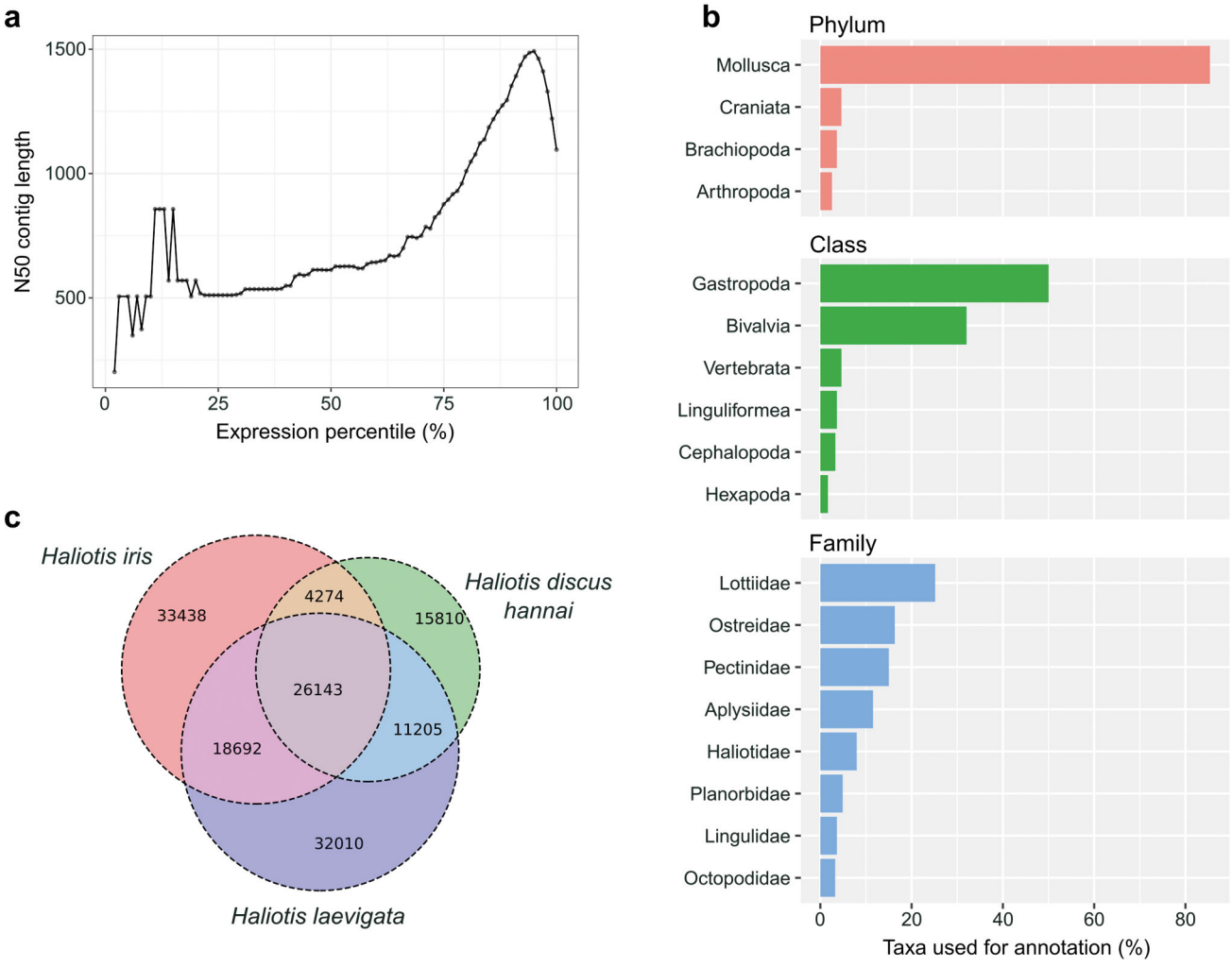

Fig. 1. (a) Transcriptome assembly quality, (b) annotation sources and (c) similarity of the *Haliotis iris* transcriptome to other *Haliotis* species. In (a), the assembly quality is measured using the 'expression N50' (ExN50), which takes into account both transcript length and expression. In (b), the taxa used for annotation were derived from the NCBI non-redundant (nr) database matches with an e-value <0.001

(Table 2, Supplement 1 at www.int-res.com/articles/suppl/d135p107_supp1.xlsx). In addition, 2 potentially stress-related genes were dysregulated, including ganglioside GM2 activator and galaxin (Table 2). At 96 h post-exposure, fewer of the differentially expressed genes were involved in chitin-binding and most were down-regulated, including genes coding for proteins involved in transportation (excitatory amino acid transporter 2 and the sodium-dependent glucose transporter 1B), neurological processes (neuroligin-4) and detoxification (cytochrome P450 3A13; Table 2).

Functionally, the up-regulated genes at 24 h post-exposure were involved in chitin metabolic pathways, and several pathways related to blood clotting, such as plasminogen activation, blood coagulation, angiotensin-activated signalling pathway and positive regulation of fibrinolysis (Table 3). Notably, the differentially expressed genes were also involved in the positive regulation of an acute inflammatory response (Table 3).

The particular up-regulated genes in this pathway were a vascular adhesion protein gene (*VAP-1*) and 2 plasma kallikreins. At 96 h post-exposure, the up-regulated pāua genes were still involved in chitin metabolism; however, they were no longer enriched for blood coagulation pathways (Table 3). In this case, the up-regulated genes were involved in the formation of an infection structure on or near the host, including 2 beta-1,4-N-acetylgalactosaminyl-transferase (*B4GALNT*) orthologues. In addition, several up-regulated genes were involved in the

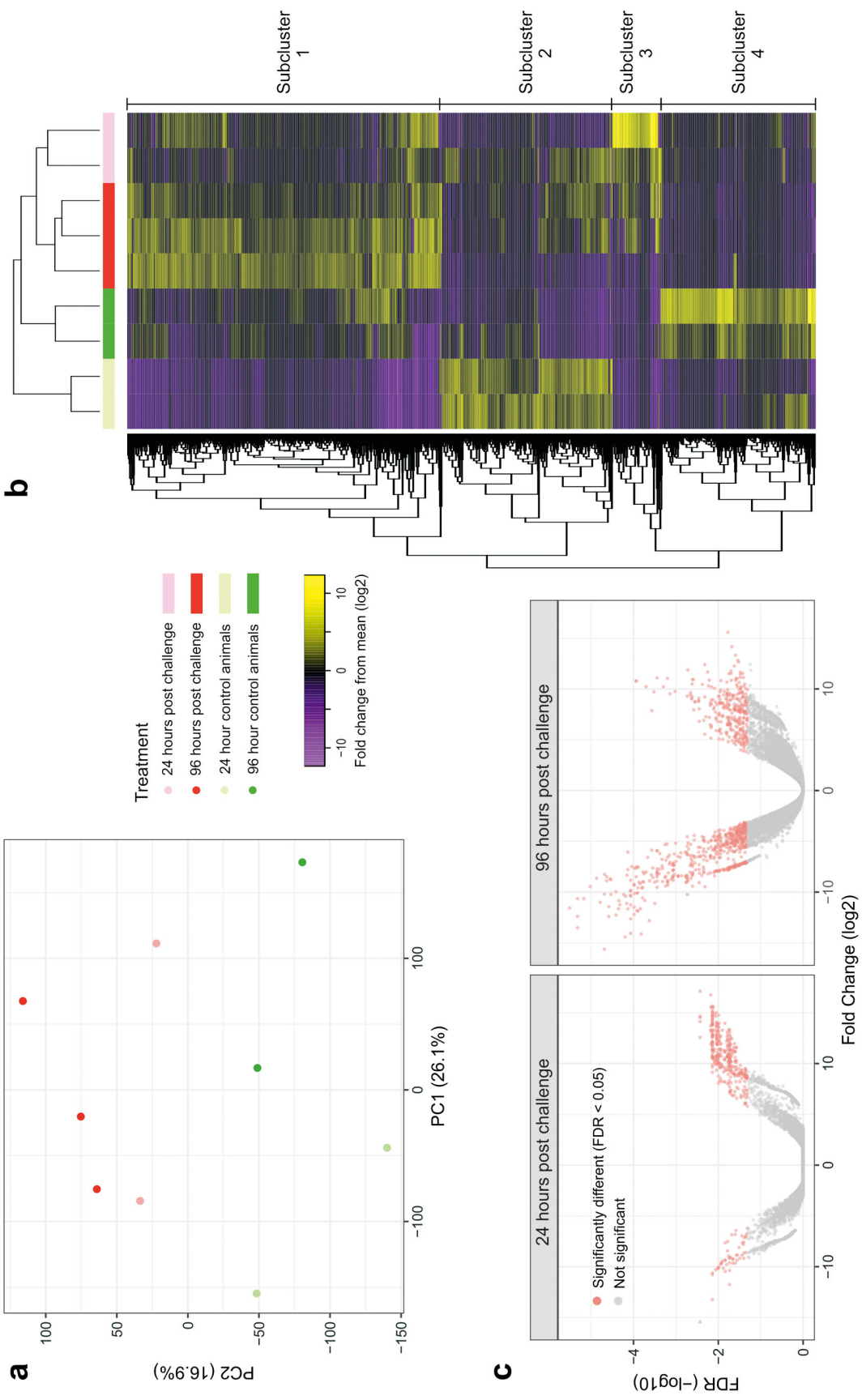

Fig. 2. Similarity of pāua (a) gene expression profiles, (b) gene co-expression patterns and (c) fold changes across the time-points, during HaHV-1-exposure and control treatments. FDR: false discovery rate adjusted p-value

Table 2. Top 10 differentially expressed genes in HaHV-1-challenged pāua. Only annotated genes are included

Gene	Fold change (log)	Corrected p	Annotation
24 h post infection			
TRINITY_DN68321_c0_g9	14.66	0.004	Chitin-binding peritrophin-A domain
TRINITY_DN28114_c0_g2	−15.45	0.004	Ganglioside GM2 activator
TRINITY_DN47043_c1_g2	17.13	0.004	Galaxin
TRINITY_DN62659_c1_g1	13.72	0.007	Protein obstructor-E
TRINITY_DN68704_c2_g5	15.56	0.007	Endochitinase
TRINITY_DN68026_c2_g2	13.22	0.007	Carbonic anhydrase 2
TRINITY_DN45501_c0_g1	16.75	0.007	Protein PIF
TRINITY_DN52722_c0_g1	13.33	0.007	Zinc metalloproteinase nas-39
TRINITY_DN64100_c0_g1	11.95	0.007	Collagen alpha-1
TRINITY_DN70118_c0_g5	14.13	0.007	Protein obstructor-E
96 h post infection			
TRINITY_DN67700_c0_g4	−9.46	<0.0001	Angiotensin-converting enzyme
TRINITY_DN56296_c0_g2	−11.00	<0.0001	POU domain, class 3, transcription factor 2-A
TRINITY_DN66908_c0_g5	−15.62	<0.0001	Perlucin containing C-type lectin domain 10
TRINITY_DN62993_c0_g2	−8.48	<0.0001	Cytochrome P450 3A13
TRINITY_DN66329_c0_g1	−11.44	<0.0001	Excitatory amino acid transporter 2
TRINITY_DN62513_c1_g1	−12.40	<0.0001	Protocadherin FAT 1
TRINITY_DN65476_c2_g1	−8.70	<0.0001	Carboxylesterase 1E
TRINITY_DN69481_c2_g3	−11.64	<0.0001	Sodium-dependent glucose transporter 1B
TRINITY_DN68966_c0_g3	−10.40	<0.0001	Homeotic protein empty spiracles
TRINITY_DN66720_c0_g2	−11.12	<0.0001	Neuroligin-4, X-linked

positive regulation of the Notch signalling pathway (Table 3). Down-regulated genes at 96 h post-exposure were generally involved in transport pathways, including sodium ion transport, amino acid transport and cobalamin transport (Table 3).

3.4. Genes containing chitin-binding peritrophin-A domains are highly up-regulated during early HaHV-1 infection

Five of the top 10 differentially expressed genes in HaHV-1-challenged pāua after 24 h contained chitin-binding peritrophin-A domains (Table 2), and the top 2 enriched functional pathways were related to chitin metabolism (Table 3). For this reason, all transcripts containing the chitin-binding peritrophin-A domain (above an expression threshold and meeting certain requirements regarding conserved cysteine positions; see Section 2.8) were analysed further (Fig. 3, Supplement 2 at www.int-res.com/articles/suppl/d135p107_supp2.pdf). The chitin-binding domains were extracted from the transcripts and aligned to visualise phylogenetic relationships and expression differences between the domains (Fig. 3). Many genes containing the conserved domain were up-regulated in pāua 24 h post-exposure compared to control pāua, although expression was less pronounced at 96 h post-exposure (Fig. 3). For example, 2 protein obstructor-E orthologues, chondroitin proteoglycan 2, an endochitinase, chitotriosidase-1, a probable chitinase 10 and protein PIF were highly up-regulated in pāua 24 h post-exposure, but their expression levels all decreased by 96 h post-exposure (Fig. 3). Interestingly, a netrin receptor was also up-regulated 24 h post-exposure (Fig. 3).

4. DISCUSSION

An abalone species from New Zealand, the blackfoot pāua, is relatively resistant to HaHV-1 infection and fully resistant to subsequent disease (Corbeil et al. 2017). To explore the genetic mechanisms that may confer resistance to pāua, we examined gene expression changes in pāua challenged with HaHV-1 at 24 and 96 h post-exposure. Although there was some intra-treatment variability in the HaHV-1-challenged pāua at 24 h post-exposure, this was likely due to the long exposure period to HaHV-1 (20 h), leading to uncertainty about when individual pāua became infected.

After infection with HaHV-1, many transcripts containing the chitin-binding peritrophin-A domain were up-regulated in the pāua. This was particularly apparent at 24 h post-exposure, but was also maintained to a lesser extent after 96 h. For instance, 2 protein obstructor-E orthologues, chondroitin pro-

Table 3. Top 10 enriched 'biological process' pathways in HaHV-1-challenged pāua. Note that too few genes were down-regulated 24 h post challenge for pathway analysis

Gene ontology term	Definition	Annotated	Significant	Expected	p
Enriched in up-regulated genes 24 h post challenge					
GO:0006030	Chitin metabolic process	167	31	0.91	<0.0001
GO:0006032	Chitin catabolic process	62	9	0.34	<0.0001
GO:0000272	Polysaccharide catabolic process	208	10	1.13	<0.0001
GO:0031639	Plasminogen activation	22	4	0.12	<0.0001
GO:0002675	Positive regulation of acute inflammatory response	23	3	0.13	<0.001
GO:2001150	Positive regulation of dipeptide transmembrane transport	5	2	0.03	<0.001
GO:0007597	Blood coagulation, intrinsic pathway	7	2	0.04	<0.001
GO:0038166	Angiotensin-activated signalling pathway	10	2	0.05	0.001
GO:0051919	Positive regulation of fibrinolysis	10	2	0.05	0.001
GO:0036233	Glycine import	40	3	0.22	0.001
Enriched in up-regulated genes 96 h post challenge					
GO:0006032	Chitin catabolic process	62	4	0.22	<0.0001
GO:0075015	Formation of infection structure on or near host	10	2	0.04	<0.001
GO:0030206	Chondroitin sulfate biosynthetic process	49	3	0.18	<0.001
GO:0000272	Polysaccharide catabolic process	208	6	0.75	<0.001
GO:0045471	Response to ethanol	237	5	0.85	0.002
GO:0006931	Substrate-dependent cell migration, cell attachment to substrate	22	2	0.08	0.003
GO:0051583	Dopamine uptake involved in synaptic transmission	23	2	0.08	0.003
GO:0032023	Trypsinogen activation	24	2	0.09	0.003
GO:0045747	Positive regulation of Notch signalling pathway	84	3	0.3	0.003
GO:0030435	Sporulation resulting in formation of a cellular spore	29	2	0.1	0.005
Enriched in down-regulated genes 96 h post challenge					
GO:0006814	Sodium ion transport	299	15	3.26	<0.0001
GO:0055085	Transmembrane transport	1557	50	16.99	<0.0001
GO:1904659	Glucose transmembrane transport	14	5	0.15	<0.0001
GO:0008203	Cholesterol metabolic process	282	13	3.08	<0.0001
GO:0097017	Renal protein absorption	7	3	0.08	<0.0001
GO:0015804	Neutral amino acid transport	112	7	1.22	<0.0001
GO:0048741	Skeletal muscle fibre development	40	5	0.44	<0.0001
GO:0043568	Positive regulation of insulin-like growth factor receptor signalling pathway	26	4	0.28	<0.001
GO:0097206	Nephrocyte filtration	13	3	0.14	<0.001
GO:0015889	Cobalamin transport	56	5	0.61	<0.001

teoglycan 2, an endochitinase, chitotriosidase-1, a probable chitinase 10 and protein PIF were highly up-regulated 24 h post-exposure and remained moderately up-regulated at 96 h. Moreover, the most enriched pathways in HaHV-1-challenged pāua at both 24 and 96 h post-exposure were chitin metabolism and chitin catabolism. Taken together, these data suggest that broad pathways involving chitin-binding domains are an important pāua defence or stress response following infection with HaHV-1.

Indeed, chitin-binding proteins are involved in the defence responses of numerous organisms and are also produced after exposure to environmental stresses, such as desiccation, saline conditions or temperature extremes (Kasprzewska 2003, Hamid et al. 2013). This was demonstrated when a species of turfgrass (*Zoysia japonica*) was genetically modified to overexpress a chitinase gene and was significantly more resistant to fungal infections compared to the wild type (Kang et al. 2017). In insects, chitin-binding proteins are a major component of a semi-permeable membrane lining the gut cavity, called the peritrophic membrane (PM) (Tetreau et al. 2015). This physical barrier is thought to protect the organism from invading pathogens (Kuraishi et al. 2011). In fruit flies, for example, a decrease in width and an increase in permeability of the PM increased the susceptibility of the flies to the pathogenic bacteria *Pseudomonas entomophilia* and *Serratia marcens* (Kuraishi et al. 2011).

Proteins containing chitin-binding domains could serve several immune roles in pāua. For example, 2 chitinase-like proteins in the Pacific oyster *Crassostrea gigas* were up-regulated in haemocytes following a challenge with bacterial lipopolysaccharide

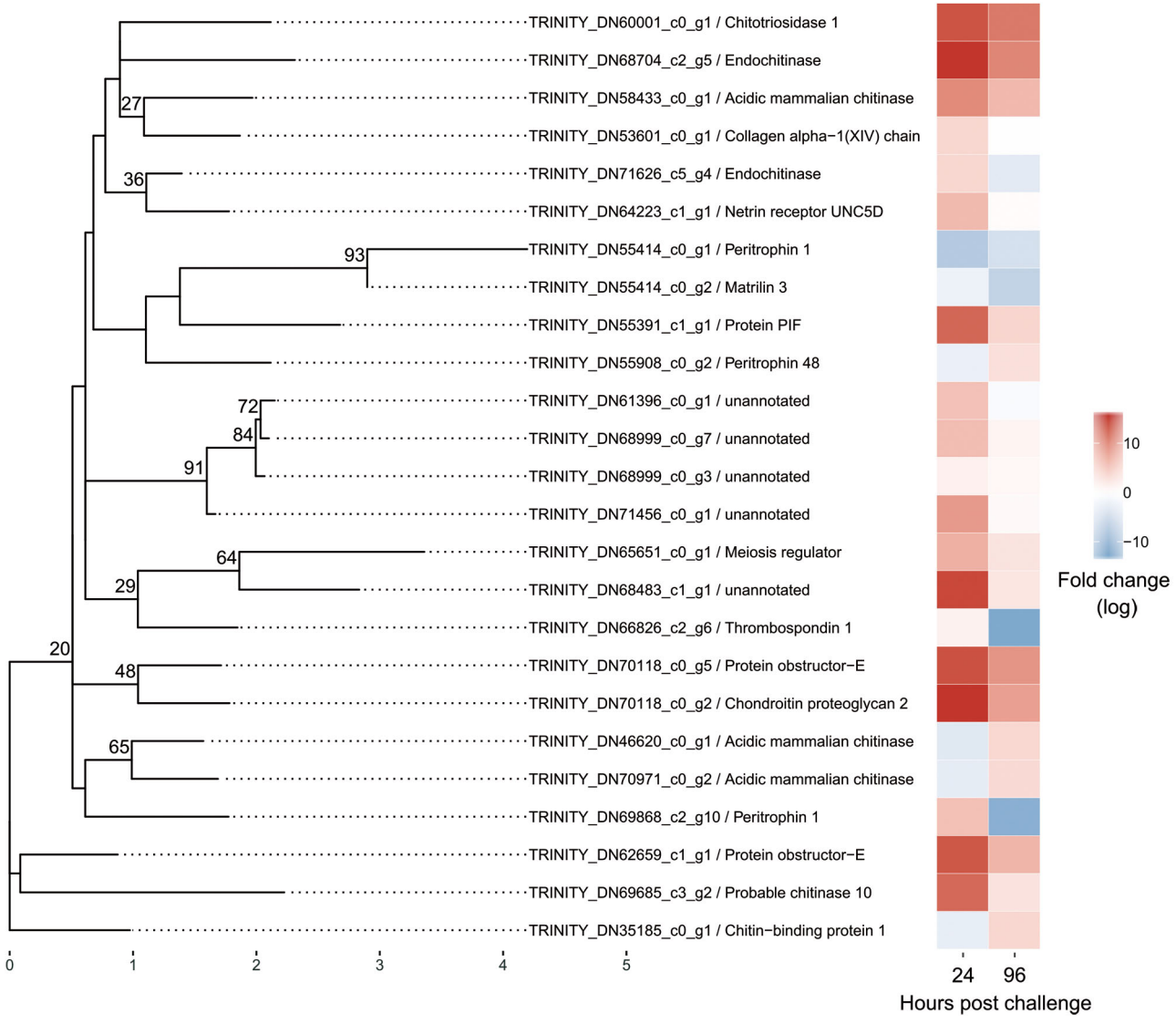

Fig. 3. Phylogenetic relationship and expression of chitin-binding peritrophin-A domains found in the pāua transcriptome. Domains were only analysed if they had an expression of 1 count per million in at least 2 replicates and had the structure '$CX_{17-20}CX_5CX_{7-22}CX_{12}CX_{6-16}C$', where C indicates conserved cysteine residues, X indicates any amino acid, and the subscript values indicate the number of spacing residues. Bootstrap values from 1000 replicates are given on the nodes if ≥20

(Badariotti et al. 2007). The authors suggested that these proteins may have roles as immune regulators or effectors (Badariotti et al. 2007). Moreover, the gastropod snail *Oncomelania hupensis* up-regulates a transcript containing a chitin-binding peritrophin-A domain when it occurs in a 'hilly' environment, and this seems to be associated with a lower infection rate of the parasitic worm *Schistosoma japonicum* (Zhao et al. 2017). Interestingly, a netrin receptor, which also contains a chitin-binding domain, was up-regulated in pāua 24 h post-exposure to HaHV-1. Netrin is known to be up-regulated during viral infections, especially during inflammatory responses. During hepatitis C infection in humans, for example, netrin-1 expression increases, which stimulates other host receptors and increases the infectivity of hepatitis C particles (Plissonnier et al. 2016). HaHV-1-challenged pāua also highly up-regulated the chitinase, chitotriosidase-1 (*CHIT1*), at both 24 and 96 h post-exposure. In mammals, *CHIT1* is largely secreted by activated macrophages and epithelial cells, and is an essential host defence response against various pathogens, including fungi and malaria (Kanneganti et al. 2012). Although an overt cellular response around nerves, similar to that seen in HaHV-1-challenged hybrid abalone, was not observed histologi-

cally in pāua. The experimental challenge was successful since the hybrid abalone showed a low viral titre 96 h post-challenge. Although viral DNA was not detected in the pāua, this is an expected result as they are relatively resistant to virus replication and may not have detectable virus DNA in their tissues at 96 h after a challenge (Corbeil et al. 2017).

It is not inconceivable that glial cells in the pāua nerves respond to HaHV-1-infection and are responsible for production of chitin-binding proteins. Overall, we detected several indications that the pāua immune response relies significantly on proteins containing chitin-binding peritrophin-A domains, which may play analogous functional roles to the chitin-binding proteins in arthropod and mammalian immune systems.

In addition to chitin-binding transcripts, the up-regulated genes in HaHV-1-challenged pāua at 24 h post-exposure were enriched for blood-clotting pathways, such as plasminogen activation, blood coagulation, angiotensin-activated signalling and positive regulation of fibrinolysis. Herpesviruses, such as HaHV-1, have long been implicated in vascular disease and are indeed capable of manipulating blood coagulation pathways. For example, herpes simplex viruses 1 and 2, and cytomegalovirus, can increase plasminogen activation in a dose-dependent manner, and enhance the rate of fibrinolysis (Gershom et al. 2010). Thus, although HaHV-1 does not cause disease in pāua, it nonetheless appears to be able to manipulate host pathways. This observation may provide insights into the stage of infection that is achieved by HaHV-1, and possibly shed light on pāua resistance mechanisms, although additional experiments are required. In addition, the up-regulated pāua genes at 24 h post-exposure were enriched for an acute inflammatory response, involving vascular adhesion protein-1 (*VAP-1*), and 2 plasma kallikreins. Vascular adhesion protein-1 is an endothelial surface glycoprotein that functions as an adhesion molecule for lymphocytes, and plays an important role in granulocyte extravasation (Tohka et al. 2001). Significantly, *VAP-1* had a log fold-change of more than 11 in HaHV-1-challenged pāua, suggesting an important immune role and a possible mechanism for viral clearance.

At 96 h post-exposure to HaHV-1, genes involved in the pathway 'formation of infection structure on or near the host' were up-regulated in the pāua, including 2 *B4GALNT* orthologues. *B4GALNT* is involved in the synthesis of GM2 ganglioside (down-regulated at 24 h post-infection, and is an important component in the central nervous system (Dad et al. 2017). Significantly, *B4GALNT* was expressed in all HaHV-1-challenged pāua, but in only 1 of the control animals. Another transcript involved in the central nervous system, neuroligin-4, was down-regulated in the pāua at 96 h post-exposure. Although the precise replication cycle for HaHV-1 in pāua is unclear, dysregulation of *B4GALNT*, GM2 ganglioside and neurolligin-4 seems to indicate that HaHV-1 is successful in reaching neurological tissues. Indeed, although disease is absent, pāua challenged with HaHV-1 by immersion do exhibit viral-infected neural cells and neuronal apoptosis (Corbeil et al. 2017), and HaHV-1 infection in other *Haliotis* species causes neurological disease (Savin et al. 2010). Moreover, positive regulation of the Notch signalling pathway was also enriched in the pāua at 96 h post-exposure. This pathway is an important cell signalling system that can be modulated by several herpesviruses. Kaposi sarcoma herpesvirus, for example, can manipulate the Notch signalling pathway by regulating the expression of several Notch ligands, thereby influencing cellular plasticity during both latent and lytic infection phases (Emuss et al. 2009). In addition, bovine herpesvirus 1 increases its survival chances during latency by expressing proteins that interfere with Notch signalling, which reduces apoptosis of infected neurons (Sinani et al. 2013). The dysregulation of these neurological and cell signalling pathways suggests that, despite the absence of disease, HaHV-1 successfully infiltrates neurological tissues in pāua. This is consistent with the *in situ* hybridization findings of Corbeil et al. (2017).

5. CONCLUSION

New Zealand pāua are naturally relatively resistant to infection by HaHV-1 and, subsequently, to the disease AVG. This resistance is in contrast to most other *Haliotis* species (Wang et al. 2004, Chang et al. 2005, Corbeil et al. 2016). In this study, we assembled the first pāua reference transcriptome and examined transcriptional changes during infection with HaHV-1 to explore the genetic mechanisms that may confer resistance to pāua. At 24 h post-exposure to the virus, pāua up-regulated broad classes of genes that contained chitin-binding peritrophin-A domains. The up-regulated chitinases may play a role as immune regulators, or, as is the case for chitotriosidase-1, may be secreted by immunologically important cells. The pāua also mounted an acute inflammatory response, including the up-regulation of transcripts coding for vascular adhesion protein-1, an important adhesion

molecule for lymphocytes in mammals. Moreover, blood coagulation pathways were broadly dysregulated in the pāua, which may have been manipulated by the virus. Finally, there were several indications that neurological tissues were affected by HaHV-1, including the dysregulation of *B4GALNT*, GM2 ganglioside, neuroligin-4 and the Notch signalling pathway. Future research into the resistance of pāua to HaHV-1 will focus on the role of chitinases, and include a detailed examination of pāua neurological tissues. Comparative gene expression studies between HaHV-1-challenged pāua and susceptible hybrid abalone, using higher animal numbers, are also imperative to perform in order to confirm the preliminary results obtained in this study. Eventually, this research may support the development of an AVG-resistant breeding programme in disease-susceptible Australian abalone and/or the development of molecular therapeutics useful to control and/or manage viral outbreaks in abalone culture.

Acknowledgements. We thank Lucy Saunders and Anton Krsinich (Craig Mostyn Group Jade Tiger Abalone Pty Ltd, Indented Head, Victoria, Australia) for providing hybrid abalone and Lynette Suvalko and Marama Cribb (Moana New Zealand Blue Abalone, Northland, New Zealand) for providing the pāua. We thank Suzanne Keeling (Ministry of Primary Industries New Zealand) for facilitating our collaboration with Moana NZ. We also thank Jenni Harper and Jean Payne from the AAHL histology laboratory for processing fixed tissue samples. Lastly, we thank Karla Helbig (LaTrobe University) for reviewing this manuscript. This work was undertaken at an NCRIS-funded facility and was funded by CSIRO.

LITERATURE CITED

Altschul SF, Gish W, Miller W, Myers EW, Lipman DJ (1990) Basic local alignment search tool. J Mol Biol 215:403–410

Badariotti F, Lelong C, Dubos MP, Favrel P (2007) Characterization of chitinase-like proteins (*Cg*-Clp1 and *Cg*-Clp2) involved in immune defence of the mollusc *Crassostrea gigas*. FEBS J 274:3646–3654

Bai CM, Rosani U, Xin LS, Li GY, Li C, Wang QC, Wang CM (2018) Dual transcriptomic analysis of Ostreid herpesvirus 1 infected *Scapharca broughtonii* with an emphasis on viral anti-apoptosis activities and host oxidative burst. Fish Shellfish Immunol 82:554–564

Bai CM, Li YN, Chang PH, Jiang JZ and others (2019) Susceptibility of two abalone species, *Haliotis diversicolor supertexta* and *Haliotis discus hannai*, to Haliotid herpesvirus 1 infection. J Invertebr Pathol 160:26–32

Bayer P (2017) orthomclToVenn 1.0. https://zenodo.org/record/840579#.XR-6SndFwjY

Benson DA, Cavanaugh M, Clark K, Karsch-Mizrachi I, Lipman DJ, Ostell J, Sayers EW (2013) GenBank. Nucleic Acids Res 41:D36–D42

Bolger AM, Lohse M, Usadel B (2014) Trimmomatic: a flexible trimmer for Illumina sequence data. Bioinformatics 30:2114–2120

Canesi L, Betti M, Ciacci C, Citterio B, Pruzzo C, Gallo G (2003) Tyrosine kinase-mediated cell signalling in the activation of *Mytilus* hemocytes: possible role of STAT-like proteins. Biol Cell 95:603–613

Chang PH, Kuo ST, Lai SH, Yang HS, Ting YY, Hsu CL, Chen HC (2005) Herpes-like virus infection causing mortality of cultured abalone *Haliotis diversicolor supertexta* in Taiwan. Dis Aquat Org 65:23–27

Chen G, Wang C, Zhang C, Wang Y, Xu Z, Wang C (2013) A preliminary study of differentially expressed genes of the scallop *Chlamys farreri* against acute viral necrobiotic virus (AVNV). Fish Shellfish Immunol 34:1619–1627

Chen G, Zhang C, Jiang F, Wang Y, Xu Z, Wang C (2014) Bioinformatics analysis of hemocyte miRNAs of scallop *Chlamys farreri* against acute viral necrobiotic virus (AVNV). Fish Shellfish Immunol 37:75–86

Chen G, Zhang C, Wang Y, Wang Y, Guo C, Wang C (2015) Molecular characterization and immune response expression of the QM gene from the scallop *Chlamys farreri*. Fish Shellfish Immunol 45:543–550

Corbeil S, Colling A, Williams LM, Wong FYK and others (2010) Development and validation of a TaqMan® PCR assay for the Australian abalone herpes-like virus. Dis Aquat Org 92:1–10

Corbeil S, McColl KA, Williams LM, Mohammad I and others (2012a) Abalone viral ganglioneuritis: establishment and use of an experimental immersion challenge system for the study of abalone herpes virus infections in Australian abalone. Virus Res 165:207–213

Corbeil S, Williams LM, Bergfeld J, Crane MSJ (2012b) Abalone herpes virus stability in sea water and susceptibility to chemical disinfectants. Aquaculture 326–329: 20–26

Corbeil S, Williams LM, McColl KA, Crane MSJ (2016) Australian abalone (*Haliotis laevigata*, *H. rubra* and *H. conicopora*) are susceptible to infection by multiple abalone herpesvirus genotypes. Dis Aquat Org 119:101–106

Corbeil S, McColl KA, Williams LM, Slater J, Crane MSJ (2017) Innate resistance of New Zealand pāua to abalone viral ganglioneuritis. J Invertebr Pathol 146:31–35

Corporeau C, Tamayo D, Pernet F, Quéré C, Madec S (2014) Proteomic signatures of the oyster metabolic response to herpesvirus OsHV-1 µVar infection. J Proteomics

Cowley JA, Corbeil S, Bulach D, Moody NJ (2012) Complete genome sequences of abalone herpesvirus (AbHV) strains from Victoria and Tasmania provide insights into its origins and identity variations useful for epidemiology. In: Elliot N (ed) 8th International Abalone Symposium, 6–11 May 2012, Hobart, Tasmania. International Abalone Society, Hobart, p 86 (Abstract)

Crane MSJ, Corbeil S, Williams LM, McColl KA, Gannon V (2013) Evaluation of abalone viral ganglioneuritis resistance among wild abalone populations along the Victorian coast of Australia. J Shellfish Res 32:67–72

Dad R, Malik U, Javed A, Minassian BA, Hassan MJ (2017) Structural annotation of beta-1,4-N-acetyl galactosaminyltransferase 1 (B4GALNT1) causing hereditary spastic paraplegia 26. Gene 626:258–263

Dang VT, Benkendorff K, Corbeil S, Williams LM, Hoad J, Crane MSJ, Speck P (2013) Immunological changes in response to herpesvirus infection in abalone *Haliotis laevigata* and *Haliotis rubra* hybrids. Fish Shellfish Immunol 34:688–691

Edgar RC (2004) MUSCLE: multiple sequence alignment with high accuracy and high throughput. Nucleic Acids Res 32:1792–1797

Emuss V, Lagos D, Pizzey A, Gratrix F, Henderson SR, Boshoff C (2009) KSHV manipulates Notch signaling by DLL4 and JAG1 to alter cell cycle genes in lymphatic endothelia. PLOS Pathog 5:e1000616

Fleury E, Huvet A (2012) Microarray analysis highlights immune response of Pacific oysters as a determinant of resistance to summer mortality. Mar Biotechnol 14: 203–217

Gerdol M, Gomez-Chiarri M, Castillo MG, Figueras A and others (2018) Immunity in molluscs: recognition and effector mechanisms, with a focus on Bivalvia. In: Cooper EL (ed) Advances in comparative immunology. Springer, Cham, p 225–341

Gershom ES, Vanden Hoek A, Sutherland MR, Pryzdial ELG (2010) Herpesviruses enhance fibrinogen clot lysis. Blood 116:1153

Grabherr MG, Haas BJ, Yassour M, Levin JZ and others (2011) Full-length transcriptome assembly from RNA-Seq data without a reference genome. Nat Biotechnol 29:644–652

Green TJ, Raftos D, Speck P, Montagnani C (2015a) Antiviral immunity in marine molluscs. J Gen Virol 96: 2471–2482

Green TJ, Speck P, Geng L, Raftos D, Beard MR, Helbig KJ (2015b) Oyster viperin retains direct antiviral activity and its transcription occurs via a signalling pathway involving a heat-stable haemolymph protein. J Gen Virol 96:3587–3597

Haas BJ, Papanicolaou A, Yassour M, Grabherr M and others (2013) De novo transcript sequence reconstruction from RNA-seq using the Trinity platform for reference generation and analysis. Nat Protoc 8:1494–1512

Hamid R, Khan MA, Ahmad M, Ahmad MM, Abdin MZ, Musarrat J, Javed S (2013) Chitinases: an update. J Pharm Bioallied Sci 5:21–29

He Y, Jouaux A, Ford SE, Lelong C, Sourdaine P, Mathieu M, Guo X (2015) Transcriptome analysis reveals strong and complex antiviral response in a mollusc. Fish Shellfish Immunol 46:131–144

Hooper C, Hardy-Smith P, Handlinger J (2007) Ganglioneuritis causing high mortalities in farmed Australian abalone (*Haliotis laevigata* and *Haliotis rubra*). Aust Vet J 85:188–193

Hunter JD (2007) Matplotlib: a 2D graphics environment. Comput Sci Eng 9:90–95

Johnson LS, Eddy SR, Portugaly E (2010) Hidden Markov model speed heuristic and iterative HMM search procedure. BMC Bioinformatics 11:431

Kang JN, Park MY, Kim WN, Kang HG and others (2017) Resistance of transgenic zoysiagrass overexpressing the zoysiagrass class II chitinase gene *Zjchi2* against *Rhizoctonia solani* AG2-2 (IV). Plant Biotechnol Rep 11:229–238

Kanneganti M, Kamba A, Mizoguchi E (2012) Role of chitotriosidase (chitinase 1) under normal and disease conditions. J Epithel Biol Pharmacol 5:1–9

Kasprzewska A (2003) Plant chitinases—regulation and function. Cell Mol Biol Lett 8:809–824

Kuraishi T, Binggeli O, Opota O, Buchon N, Lemaitre B (2011) Genetic evidence for a protective role of the peritrophic matrix against intestinal bacterial infection in *Drosophila melanogaster*. Proc Natl Acad Sci USA 108: 15966–15971

Langmead B, Salzberg SL (2012) Fast gapped-read alignment with Bowtie 2. Nat Methods 9:357–359

Li B, Dewey CN (2011) RSEM: accurate transcript quantification from RNA-Seq data with or without a reference genome. BMC Bioinformatics 12:323

Li H, Handsaker B, Wysoker A, Fennell T and others (2009) The Sequence Alignment/Map format and SAMtools. Bioinformatics 25:2078–2079

Li L, Stoeckert CJ, Roos DS (2003) OrthoMCL: identification of ortholog groups for eukaryotic genomes. Genome Res 13:2178–2189

Martín-Gómez L, Villalba A, Kerkhoven RH, Abollo E (2014) Role of microRNAs in the immunity process of the flat oyster *Ostrea edulis* against bonamiosis. Infect Genet Evol 27:40–50

Nam BH, Kwak W, Kim YO, Kim DG and others (2017) Genome sequence of Pacific abalone (*Haliotis discus hannai*): the first draft genome in family Haliotidae. Gigascience 6:1–8

Normand J, Li R, Quillien V, Nicolas JL, Boudry P, Pernet F, Huvet A (2014) Contrasted survival under field or controlled conditions displays associations between mRNA levels of candidate genes and response to OsHV-1 infection in the Pacific oyster *Crassostrea gigas*. Mar Genomics 15:95–102

OIE (World Organisation for Animal Health) (2017) Infection with abalone herpesvirus. www.oie.int/index.php?id=2439&L=0&htmfile=chapitre_abalone_herpesvirus.htm

Plissonnier ML, Lahlali T, Michelet M, Lebossé F and others (2016) Epidermal growth factor receptor-dependent mutual amplification between Netrin-1 and the Hepatitis C virus. PLOS Biol 14:e1002421

Punta M, Coggill P, Eberhardt R, Mistry J and others (2012) The Pfam protein families databases. Nucleic Acids Res 40:D290–D301

Robinson MD, McCarthy DJ, Smyth GK (2010) edgeR: a Bioconductor package for differential expression analysis of digital gene expression data. Bioinformatics 26:139–140

Rosani U, Varotto L, Domeneghetti S, Arcangeli G, Pallavicini A, Venier P (2015) Dual analysis of host and pathogen transcriptomes in ostreid herpesvirus 1-positive *Crassostrea gigas*. Environ Microbiol 17:4200–4212

Savin KW, Cocks BG, Wong F, Sawbridge T, Cogan N, Savage D, Warner S (2010) A neurotropic herpesvirus infecting the gastropod, abalone, shares ancestry with oyster herpesvirus and a herpesvirus associated with the amphioxus genome. Virol J 7:308

Seo JK, Go HJ, Kim CH, Nam BH, Park NG (2016) Antimicrobial peptide, hdMolluscidin, purified from the gill of the abalone, *Haliotis discus*. Fish Shellfish Immunol 52: 289–297

Sinani D, Frizzo da Silva L, Jones C (2013) A bovine herpesvirus 1 protein expressed in latently infected neurons (ORF2) promotes neurite sprouting in the presence of activated Notch1 or Notch3. J Virol 87:1183–1192

Stamatakis A (2014) RAxML version 8: a tool for phylogenetic analysis and post-analysis of large phylogenies. Bioinformatics 30:1312–1313

Tan J, Lancaster M, Hyatt A, van Driel R, Wong F, Warner S (2008) Purification of a herpes-like virus from abalone (*Haliotis* spp.) with ganglioneuritis and detection by transmission electron microscopy. J Virol Methods 149: 338–341

Tetreau G, Dittmer NT, Cao X, Agrawal S and others (2015) Analysis of chitin-binding proteins from *Manduca sexta*

provides new insights into evolution of peritrophin A-type chitin-binding domains in insects. Insect Biochem Mol Biol 62:127–141

The UniProt Consortium (2017) UniProt: the universal protein knowledgebase. Nucleic Acids Res 45: D158–D169

Tohka S, Laukkanen M, Jalkanen S, Salmi M (2001) Vascular adhesion protein 1 (VAP-1) functions as a molecular brake during granulocyte rolling and mediates recruitment in vivo. FASEB J 15:373–382

Wang JY, Guo ZX, Feng J, Liu GF, Xu LW, Chen BS, Pan JP (2004) Virus infection in cultured abalone, *Haliotis diversicolor* Reeve in Guangdong Province, China. J Shellfish Res 23:1163–1168

Wickham H (2016) ggplot2: elegant graphics for data analysis. Springer-Verlag, New York, NY

Yu G, Smith DK, Zhu H, Guan Y, Lam TTY (2017) Ggtree: an R package for visualization and annotation of phylogenetic trees with their covariates and other associated data. Methods Ecol Evol 8:28–36

Zhao JS, Wang AY, Zhao HB, Chen YH (2017) Transcriptome sequencing and differential gene expression analysis of the schistosome-transmitting snail *Oncomelania hupensis* inhabiting hilly and marshland regions. Sci Rep 7:15809

Zhuang J, Coates CJ, Zhu H, Zhu P, Wu Z, Xie L (2015) Identification of candidate antimicrobial peptides derived from abalone hemocyanin. Dev Comp Immunol 49:96–102

Editorial responsibility: Stewart Johnson, Nanaimo, British Columbia, Canada

Submitted: January 14, 2019; Accepted: June 14, 2019
Proofs received from author(s): July 24, 2019